Effects of deposition parameters on the optical and microstructural characteristics of sputtered deposited nanocrystalline ZnO thin films

D. Cornejo Monroy and J. F. Sánchez-Ramírez
Centro de Investigación en Ciencia Aplicada y Tecnología Avanzada,
Instituto Politécnico Nacional,
Legaría # 694, Col. Irrigación, 11500 México D.F., Mexico.

M. Herrera-Zaldívar
Centro de Ciencias de la Materia Condensada, Universidad Nacional Autónoma de México,
Apartado postal 2681, Ensenada, B. C, 22800, Mexico.

U. Pal*
Instituto de Física, Universidad Autónoma de Puebla,
Apartado Postal J-48, Puebla, Pue. 72570, Mexico,
e-mail: upal@sirio.ifuap.buap.mx

Nanocrystalline ZnO thin films were deposited on silicon and quartz substrates at different working pressures and different r.f. powers to study their structural and optical properties. The films were characterized by X-ray diffraction (XRD), scanning electron microscopy (SEM) and optical absorption spectroscopy techniques. The ZnO films were of polycrystalline nature with very small grain size. All the ZnO films were of hexagonal wurtzite structure. While the microstructural characteristics of the films depended strongly on the deposition parameters, their optical properties did not vary significantly. Films deposited at higher working pressures were of bigger grain size, irrespective of the nature of the substrate. In general, increase of r.f. power decreases the negative stress in the films.

Keywords: ZnO thin films; r.f. sputtering; microstructures; optical properties.

Películas delgadas nanocristalinas de ZnO fueron depositadas sobre substratos de cuarzo y silicio a diferentes presiones de trabajo y diferentes potencias r.f. para estudiar sus propiedades estructurales y ópticas. Las películas fueron caracterizadas utilizando las técnicas de difracción de rayos-X, microscopia electrónica de barrido y espectroscopia de absorción óptica. Las películas de ZnO son policristalinas con tamaño de grano muy pequeño. Todas las películas de ZnO presentan estructura hexagonal tipo wurtzita. Mientras las características microestructurales de las películas dependen fuertemente sobre los parámetros de deposición, sus propiedades ópticas no varían significativamente. Películas depositadas a mayores presiones de trabajo presentan mayores tamaños de grano independientemente del tipo de substrato. En general, un incremento de la potencia r.f. decrece la tensión negativa en las películas.

Descriptores: Películas delgadas de ZnO; espurreo r.f.; microestructuras; propiedades ópticas.

PACS: 61.72.-y; 68.47.Gh; 78.20.-e; 78.66.-w

1. Introduction

Zinc oxide (ZnO) is an important electronic and photonic material because of its wide direct band gap of 3.37 eV and large exciton binding energy of 60 meV at room temperature. This strong exciton binding energy, which is much larger than the thermal energy (26 meV at RT), can ensure an efficient UV-blue emission at room temperature. Consequently, thin films of ZnO became one of the most important functional materials with unique properties of near-UV emission, optical transparency, electrical conductivity, and piezo electricity. Extensive applications of ZnO in various areas, such as gas sensors [1], power devices [2], UV-light-emitting diodes [3], photocatalysis [4], solar cell [5], and CMOS-chip-integrated micro-phones [6] are further enhanced on reduction of its size, *i.e.* from bulk to nanoscale [4]. Of the various thin film deposition techniques [7-14], magnetron sputtering [15,16] is a popular technique to prepare thin films with high deposition rates onto a large area. Sputtering parameters such as working gas pressure, substrate temperature, and sputtering power play important roles in controlling the properties of the films. In the present investigation, we prepared ZnO thin films on quartz and silicon (Si) substrates by radio frequency (r.f.) magnetron sputtering and studied the influence of deposition parameters like the type of substrate, working pressure and r.f. power on their structure and optical properties.

2. Experimental

ZnO thin films were deposited on silicon and quartz substrates at different working pressures and with different powers by r.f. magnetron sputtering at room temperature as presented in Table I. The quartz substrates were cleaned in trichloroethylene, acetone and methanol using ultrasonic treatment and rinsed in deionized water. Si (100) substrates (Crysteco) were first cleaned in a hot H_2O_2-H_2SO_4 (1:1) mixture and then in 0.5% HF solution and deionized water. A 5.0 cm diameter ZnO (99.999%) target was used for film deposition and argon was used as the plasma forming gas. The argon gas flow rate was controlled at 5 ml/min. Before

the deposition of thin films, the target was pre-sputtered for about 15 minutes. Keeping the target - substrate distance at 3 cm, the ZnO films were deposited for 2 hr. 30 min. Thicknesses of the films were measured using an Alpha-Step 300 (Tencor Instruments) profilometer. The microstructure of the films was studied by a Phillips X'Pert X-ray diffractometer using CuK$_\alpha$ (with λ=1.5406 Å) radiation and scanning electron microscopy (SEM, JEOL JSM 5300) with analytical system attached. The optical absorption spectra of the films were recorded using a UV-VIS-NIR double beam spectrophotometer (SHIMADZU 3101PC).

3. Results and discussion

The X-ray diffraction spectra of the ZnO films deposited on Si and quartz substrates at different growth conditions are shown in Figs. 1 and 2, respectively. The XRD patterns of the films deposited on silicon substrates (Fig. 1) revealed diffrac-

TABLE I. Processing parameters and properties of the ZnO thin films deposited by r.f. sputtering.

Sample	Substrate	RF Power (W)	Working Pressure (mbar)	Thickness (Å)	Calculated Band Gap (eV)	d spacing (Å)	Calculated Grain Size (Å)	X-ray Density (g/cm^3)	C$_{film}$ (Å)	Stress (Gpa)
ZnO/Si-1	Silicon	150	5×10^{-2}	–	–	2.627	82	5.624	5.254	-1.577
ZnO/Si-2	Silicon	150	1×10^{-1}	–	–	2.621	90	5.636	5.242	-1.344
ZnO/Si-3	Silicon	275	5×10^{-2}	–	–	2.618	87	5.643	5.236	-1.457
ZnO/Si-4	Silicon	275	1×10^{-1}	–	–	2.622	96	5.634	5.244	-1.183
ZnO/Quartz-1	Quartz	150	5×10^{-2}	1429	3.293	2.648	76	5.580	5.296	-3.334
ZnO/Quartz-2	Quartz	150	1×10^{-1}	856	3.295	2.629	85	5.619	5.258	-1.580
ZnO/Quartz-3	Quartz	275	5×10^{-2}	3052	3.302	2.643	93	5.589	5.286	-3.989
ZnO/Quartz-4	Quartz	275	1×10^{-1}	1884	3.315	2.623	135	5.632	5.246	-1.449
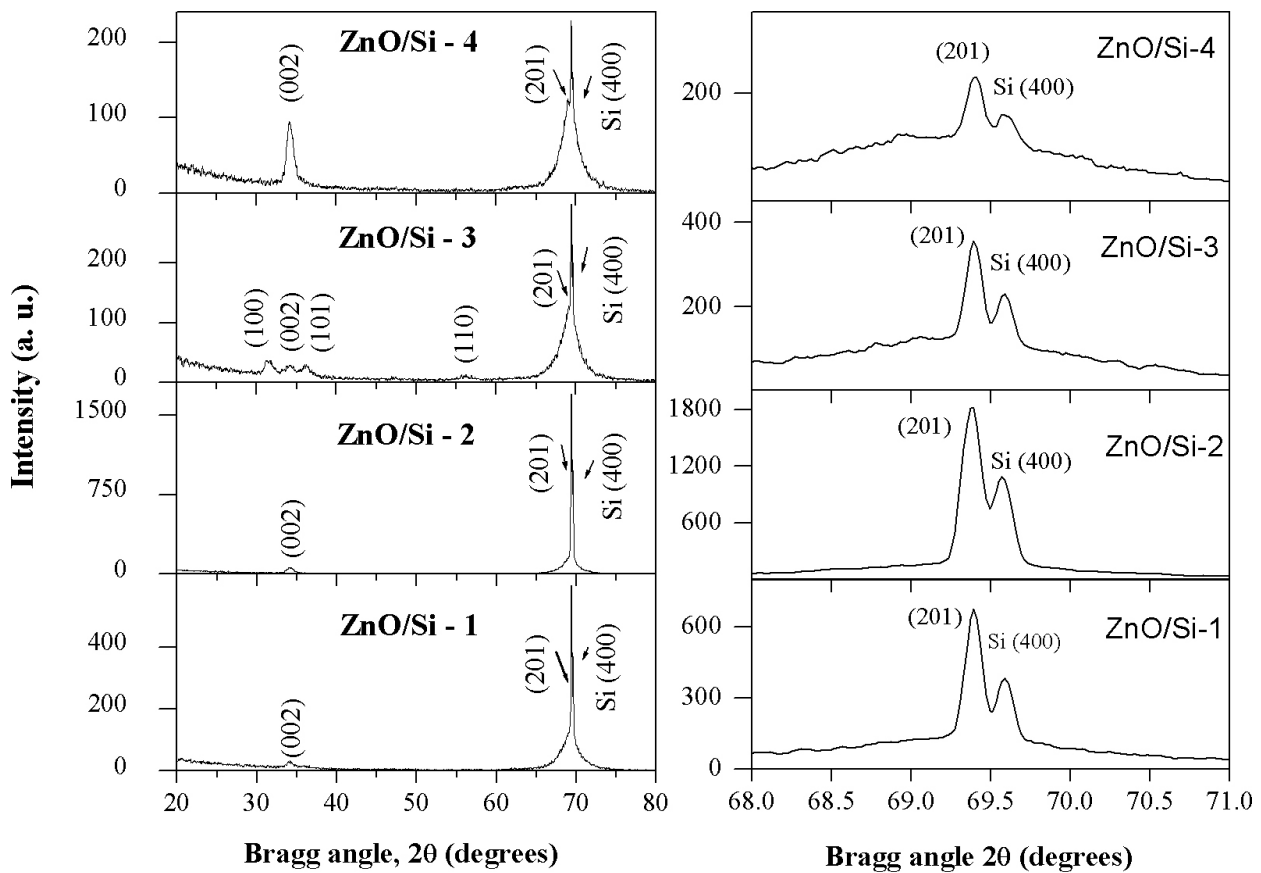
FIGURE 1. XRD patterns of r.f. sputtered ZnO films deposited on Si substrates. To visualize the Si (400) peak clearly, the corresponding angular range is amplified and shown at right.

tion peaks of ZnO in hexagonal wurtzite phase together with a sharp peak of the Si substrate. Films grown with 150 W r.f. power exhibited two peaks correspond to (002) and (201) planes of ZnO. The intensity of these peaks increased with the increase of work pressure, improving the crystallinity of the films. The samples denominated as ZnO/Si-3 and ZnO/Si-4 are the films deposited on silicon with 275 W of r.f. power. Of these samples, the film deposited at 275 r.f. power and 5×10^{-2} mbar work pressure (ZnO/Si-3), there appeared 5 peaks of week intensity. However, the film deposited at 1×10^{-1} mbar with 275 r.f. power revealed only two intense peaks of wurtzite ZnO. The appearance of only two peaks (002) and (201), in ZnO/Si-4 sample indicates that the films deposited on silicon tend to align themselves preferentially on the substrate (along c-axis) when deposited at higher work pressure. As the surface energy density of the (002) orientation is the lowest in a ZnO crystal, (002) orientation is favored in the film [17].

The XRD patterns obtained from thin films deposited on quartz substrates are shown in Fig. 2. As shown in the figure, the films grown with 150 W r.f. power are mostly amorphous. On increasing the work pressure, the crystallinity of the films increased. The crystallinity of the films deposited at higher r.f. power is better than the films deposited at lower r.f. power. Again, the films grown preferentially along [002] direction while deposited at higher work pressure. The interplaner spacing d values of the films were calculated for the (002) plane using Bragg's relation and presented in Table I.
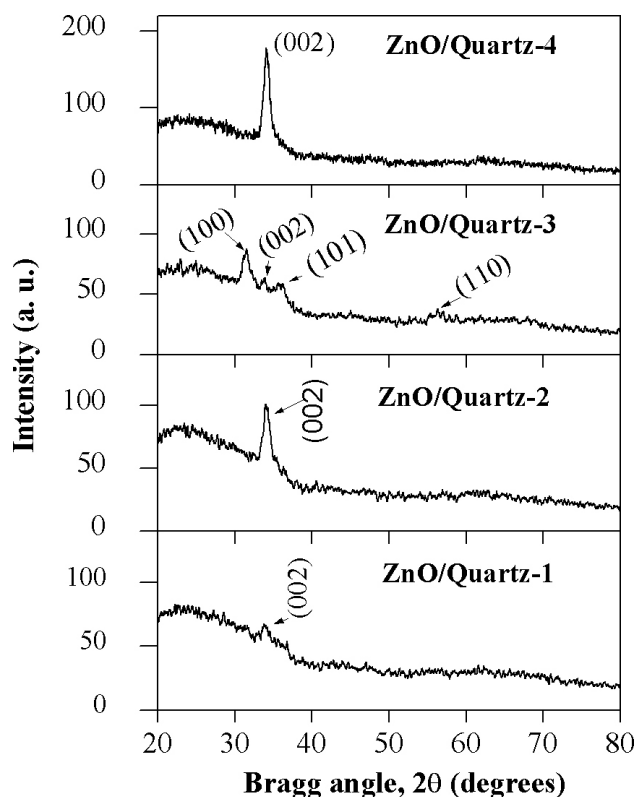
The d values obtained for all the films are higher with respect to its standard values [18]. The d values decreased with the increase of r.f. power. Higher values of d in our films in comparison with the bulk (2.604 Å, JCPDS file no. 36-1451) or in other words, higher lattice constant C_{film} values (5.239- 5.304 Å) in comparison with its bulk counterpart ($C_{\text{bulk}} = 5.208$ Å) suggests an elongation of unit cells along the c-axis, and existence of compressive stresses along the plane of the films.

To derive the stress σ_{film} parallel to the surface in hexagonal lattice, we used the equation [19]:

$$\sigma_{\text{film}} = [2C_{13}^2 - C_{33}(C_{11} + C_{12})]\frac{(C_{\text{film}} - C_{\text{bulk}})}{(2C_{13}C_{\text{bulk}})}, \quad (1)$$

where c_{ij} are the elastic constants; C_{film} and C_{bulk} are the lattice constants of the film and bulk, respectively. C_{ij} data for single crystal ZnO have been used as C_{11}=209.7 Gpa, C_{33}=210.9 GPa, C_{12}=121.1 GPa and C_{13}=105.1 Gpa [20]. This yields the following numerical relation for the stress derived from XRD results:

$$\sigma_{\text{film}} = -226.8\text{GPa}\frac{(C_{\text{film}} - C_{\text{bulk}})}{C_{\text{bulk}}}. \quad (2)$$

The calculated d spacing and stress for the films are listed in Table I. All the films have negative stress, indicating that the lattice constant C is elongated. In order to estimate the density of a unit cell of ZnO thin film by X-ray analysis, we used the relation [21]:

$$X - \text{ray density} = \frac{M}{N * V}, \quad (3)$$

where M is the total mass in a unit cell of ZnO; N is the Avogadro number, and V is the volume of the unit cell. Considering the bulk lattice parameter a value [22], we calculated the density for all the films in the range of 5.580-5.643 g/cm^3, which are lower than the value for unstressed ZnO powder (5.674 g/cm^3). Such a lower density of unit cells in our films is believed to be due to stress-induced elongation of unit cell.

Using Scherrer relation [23], the average grain size in the films were estimated from their XRD patterns and presented in Table I. From the table, it can be seen that the thickness of the ZnO films decreased with the increase of work pressure and increased with the increase of r.f. power. When the sputtering pressure increased from 5×10^{-2} mbar to 1×10^{-1} mbar, the mean free path of the sputtered particles decreased. On increasing the sputtering pressure, during traveling from the target to substrate, the sputtered particles suffer more collisions, and some of the sputtered particles were back scattered towards the target. This resulted in a decrease of the deposition rate due to scattering. The decrease of r.f. power also result a decrease of sputtering rate causing a decrease in film thickness.

The grain size of the films increased with the increase of sputtering pressure due to improvement in the degree of crystallinity of the films, which is directly related with a slower

FIGURE 2. XRD patterns of r.f. sputtered ZnO films deposited on quartz substrates.

deposition rate at lower work pressure. A similar observation has also been made by Subramanyam *et al.* [24] for their sputtered deposited ZnO films. The better orientation of the films is also related to the slower deposition rate. Due to single crystalline nature of the Si substrate used in the present work, the ZnO films grown on them at lower work pressure oriented preferentially. However, for a particular work pressure, the particle size increased with the increase of r.f. power, which might be due to higher film thickness in them.

Typical SEM micrographs of the ZnO film surfaces, deposited on Si are shown in Fig. 3. Surfaces without some special characteristic feature are predominant and indicate a uniform growth with small grain size. Similar results are obtained for the other films deposited on quartz substrates (Fig. 4).
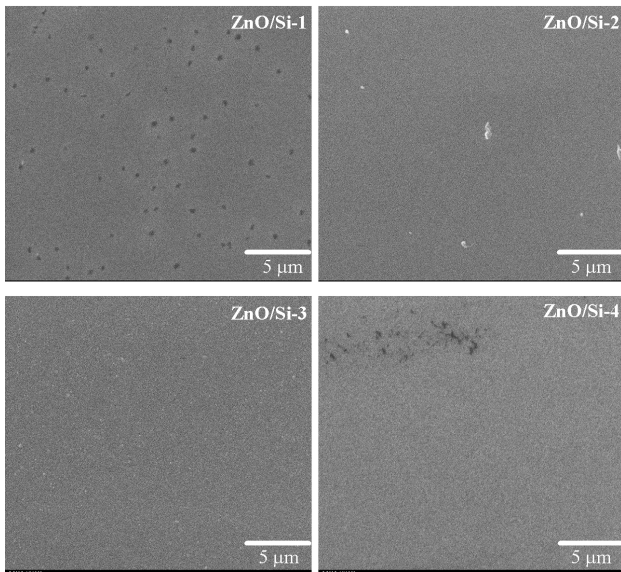
FIGURE 3. Typical top view SEM micrographs of ZnO thin films deposited on silicon substrates.
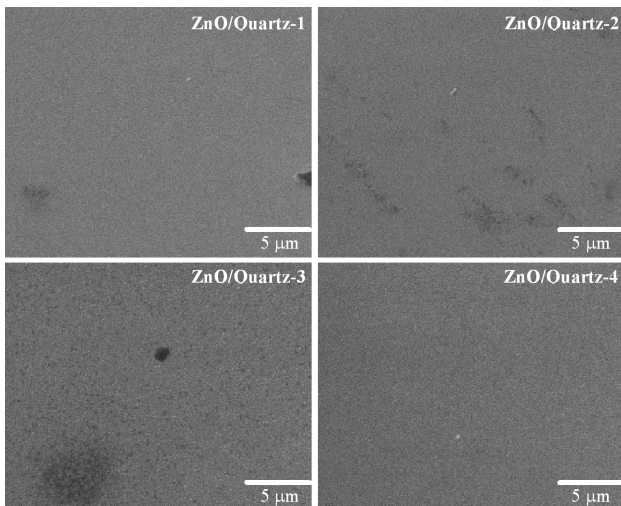
FIGURA 4. Typical top view SEM micrographs of ZnO thin films deposited on quartz substrates.
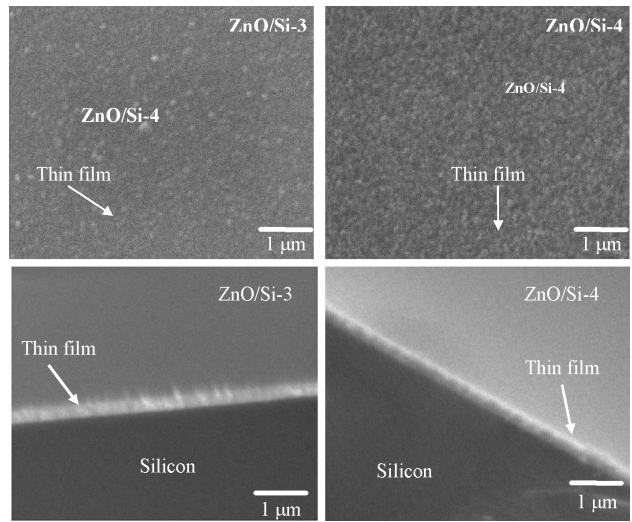
FIGURE 5. Typical SEM micrographs of ZnO thin films deposited on Si: (a) amplified top views, and (b) cross-sections.
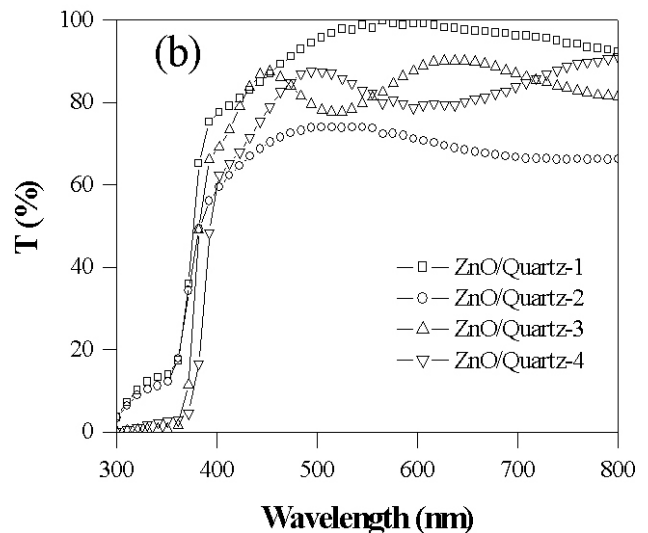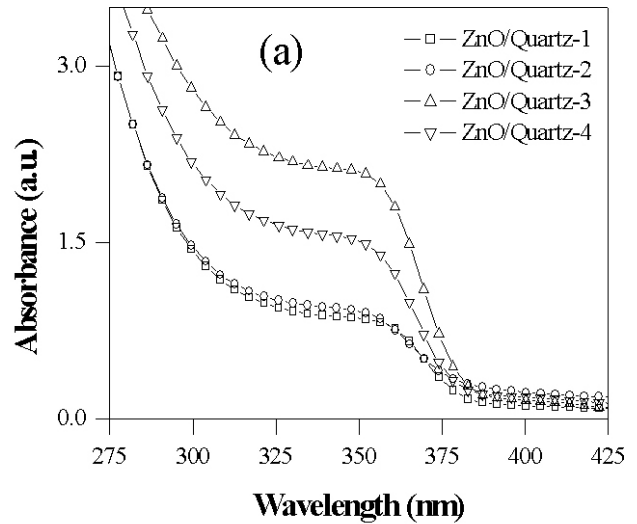
FIGURE 6. Optical absorption (a) and transmittance (b) spectra of thin films deposited on quartz substrates.
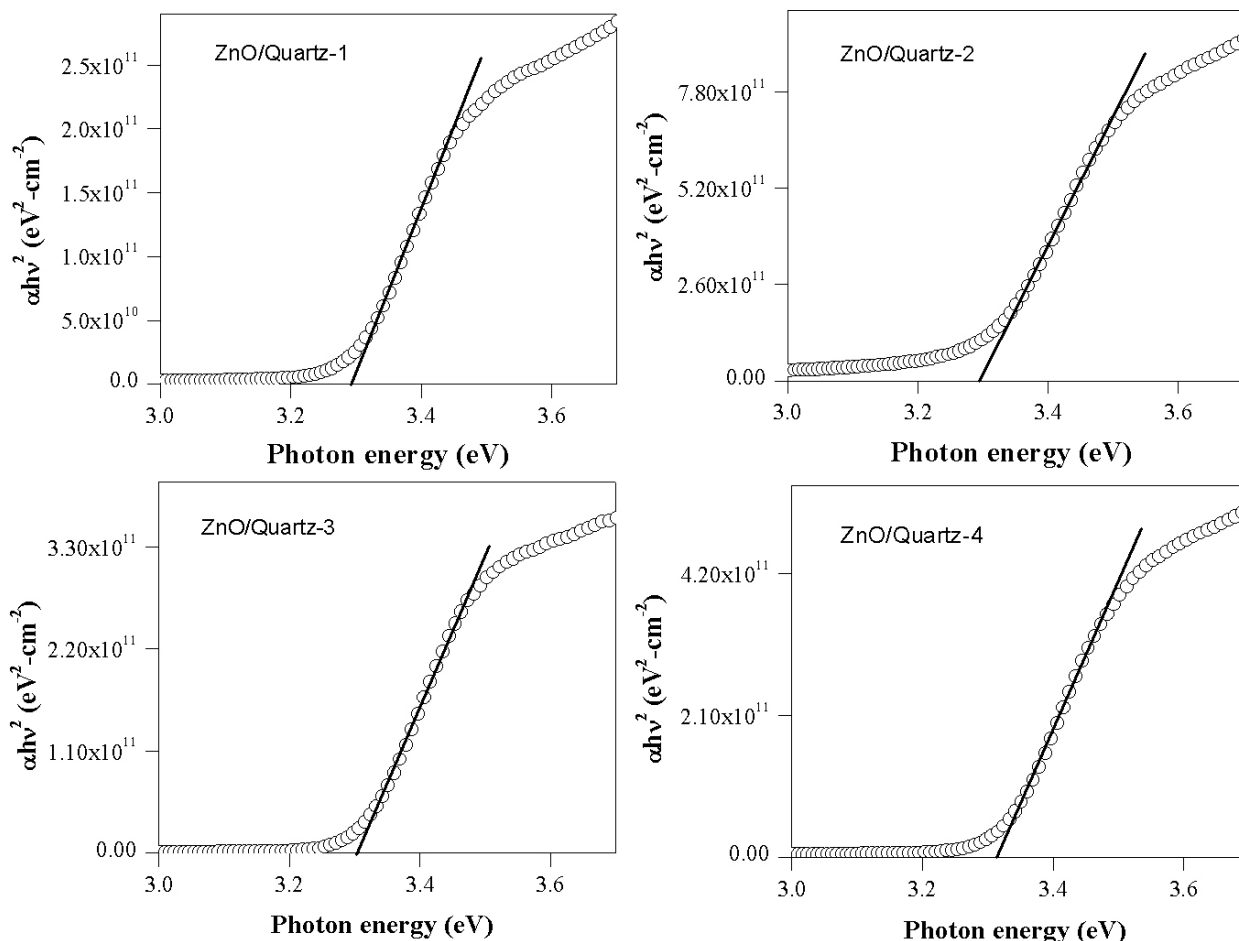
FIGURE 7. $(\alpha h\nu)^2$ vs. $(h\nu)$ plots for the ZnO thin films on quartz substrates.

In the Fig. 5a, high magnification SEM images of the samples grown on Si substrates are shown. From the micrographs we can observe the formation of nanometer size grains in the films. While the formation of nanometric particles in the samples is clear in the micrographs, exact determination of particle size from them was not possible.

In Fig. 5b, typical cross-sectional SEM micrographs for the samples ZnO/Si-3 and ZnO/Si-4 deposited at 275 W r.f. power are shown. The morphology of both the samples is uniform. For the sample ZnO/Si-3, it is possible to appreciate the growth of columnar structures of the film deposited on silicon substrate. This characteristic is not very clear in the sample ZnO/Si-4. Similar results were obtained for the other films deposited on Si. The average grain size values for all the films were evaluated from their XRD patterns using the Scherrer relation [23], and are presented in Table I.

The optical absorption and transmittance spectra for the films deposited on quartz substrates at different deposition conditions are shown in Fig. 6. The films are highly transparent in the visible spectral region (Fig. 6b). The variation of absorption coefficient α, with photon energy $(h\nu)$ was found to obey the relation $(\alpha h\nu)=A(h\nu t E_g p)^{1/2}$ (for allowed direct transition), where A is a constant and E_g is the optical band gap, indicating a direct band gap nature of the samples. The

optical band gap values are obtained by extrapolating the linear portions of the plots of $(\alpha h\nu)^2$ vs. $h\nu$ The variation of $(\alpha h\nu)^2$ with $h\nu$ or the films formed on quartz substrate under different growth conditions are shown in Fig. 7. It is observed that the values of E_g do not change much from sample to sample. However, the estimated gap values are a bit lower than the reported band gap value of ZnO bulk (3.37 eV). The optical band gap of the films increased from 3.29 to 3.32 eV on increasing the r.f. power from 150 W to 275 W. The band gap values obtained for our samples are in good agreement with the reports on ion beam sputtered [25] and ultrasonically sprayed [26] films.

4. Conclusions

In conclusion, nanocrystalline ZnO thin films have been deposited onto quartz and silicon substrates by r.f. magnetron sputtering technique at different deposition conditions. The r.f. power and working pressure play prominent roles on the morphology, structure and optical properties of the films. All the films grow in hexagonal wurtzite phase. The crystallinity of the films is better when they are deposited at lower r.f. power and high working pressure, irrespective of the nature of the substrates. The average grain size of the films is big-

ger when they are deposited on Si substrates at high working pressure and low r.f. powers, and smaller when they are deposited on quartz substrates. The ZnO films deposited in this work are negatively stressed due to elongation of lattice constant c. Variation of the deposition parameters is seen to have no appreciable effect on the optical band gap of the films.

Acknowledgement

1. G. Sberveglieria, S. Groppellia, P. Nellia, A. Tintinellib, and G. Giuntab, *Sens. Actuators B* **25** (1995) 588.

2. T.P. Chow, and R. Tyagi, *IEEE Trans. Electron Devices* **41** (1994) 1481.

3. H. Ohta, K. Kawamura, M. Orita, N. Sarukura, M. Hirano, and H. Hosono, *Electron. Lett.* **36**(2000) 984.

4. H. Yumoto, T. Inoue, S.J. Li, T. Sako, and K. Nishiyama, *Thin Solid Films* **345**(1999) 38.

5. N. Golego, S.A. Studenikin, and M. Cocivera, *J. Electrochem. Soc.* **147** (2000) 1592.

6. S. S. Lee, R. P. Ried, and R. M. White, *J. Microelectromech. Syst.* **5** (1996) 238.

7. B.D. Yao, Y.F. Chan, and N. Wang, *Appl. Phys. Lett.* **81** (2002) 757.

8. J. Lee, M. Kang, S. Kim, M. Lee, and Y. Lee, *J. Cryst. Growth.* **249** (2003) 201.

9. J. Zhong, S. Muthukumar, Y. Chen, Y. Lu, H.M. Ng, W. Jiang, anf E.L. Garfunkel, *Appl. Phys. Lett.* **83** (2003) 3401.

10. M.H. Huang, Y. Wu, H. Feick, N. Tran, E. Weber, and P. Yang, *Adv. Mater.* **13** (2001) 113.

11. N. Saito, H. Haneda, T. Sekiguchi, N. Ohashi, I. Sakaguchi, and K. Koumoto, *Adv. Mater.* **14** (2002) 418.

12. Y.C. Kong, D.P. Yu, B. Zhang, W. Fang, S.Q. Feng, *Appl. Phys. Lett.* **78** (2001) 407.

13. Y. Li, G.W. Meng, L.D. Zhang, and F. Phillipp, *Appl. Phys. Lett.* **76** (2000) 2011.

14. Y.W. Heo, V. Varadarajan, M. Kaufman, K. Kim, D.P. Norton, F. Ren, and P.H. Fleming, *Appl. Phys. Lett.* **81** (2002) 3046.

15. A. Hachigo, H. Nakahata, K. Higaki, S. Fujii, and S. Shikata, *Appl. Phys. Lett.* **65** (1994) 2556.

16. J.G.E. Gardeniers, Z.M. Rittersma, and G.J. Burger, *J. Appl. Phys.* **83** (1998) 7844.

17. M.K. Jayaraj, A. Antony, and M. Ramachandra, *Bull. Mater. Sci.* **25** (2002) 227.

18. V. Gupta, A. Mansingh, *J. Appl. Phys.* **80** (1996) 1063.

19. R. Cebulla, R. Wendt, and K. Ellmer, *J. Appl. Phys.* **83** (1998) 1087.

20. T.B. Bateman, *J. Appl. Phys.* **33** (1962) 3309.

21. B.D. Cullity, *Elements of X-Ray Diffraction*, 2 ed (Addison-Wesley, Mass., 1978), Chap. 3.

22. V. Gupta, and A. Mansingh, *J. Appl. Phys.* **80** (1996) 1063.

23. P. Scherrer, *Nachr. Ges. Wiss. Göttingen* **2** (1918) 98.

24. T.K. Subramanyam, B.S. Naidu, S. Uthanna, *Cryst. Res. Technol.* **35** (2000) 1193.

25. Y. Qu, T. A. Gessert, T.J. Coutts, and R. Noufi, *J. Vac. Sci. Technol. A* **12** (1994) 1507.

26. T.Y. Ma, S.H. Kim, H.Y. Moon, G.C. Park, Y.J. Kim, K.W. Kim, *Jpn. J. Appl. Phys.* **35** (1996) 6208.